ELSEVIER

Infrared Physics & Technology 38 (1997) 133–138

INFRARED PHYSICS
& TECHNOLOGY

A spectroscopic study of GaAs homojunction internal photoemission far infrared detectors

W.Z. Shen [a,*], A.G.U. Perera [a], S.K. Gamage [a], H.X. Yuan [a,1], H.C. Liu [b], M. Buchanan [b], W.J. Schaff [c]

[a] *Department of Physics and Astronomy, Georgia State University, Atlanta, GA 30303, USA*
[b] *Institute for Microstructural Sciences, National Research Council, Ottawa, Canada K1A 0R6*
[c] *School of Electrical Engineering, Cornell University, Ithaca, NY 14853, USA*

Received 6 January 1997

Abstract

We report a spectroscopic study of absorption and photoconductivity in GaAs homojunction interfacial workfunction internal photoemission (HIWIP) far-infrared (FIR) detectors utilizing molecular beam epitaxy (MBE) grown multilayer (p^+–p^-–p^+–p^- ...) structures. Strong FIR (50–200 μm) free carrier absorption has been observed and analyzed for a p^+ GaAs thin film, revealing the suitability for FIR detection. The basic physical mechanism of free carrier absorption in the HIWIP FIR detectors has been determined to be an acoustic phonon-emission assisted process. A simple recombination model is proposed to account for the bias dependence of the responsivity and the saturation behavior. Using the measured responsivity and dark current data, detectivity (D_λ^*) of the FIR detectors has also been estimated. © 1997 Elsevier Science B.V.

PACS: 78.66.Fd; 72.40.+W; 85.60.Gz

1. Introduction

The idea of internal photoemission detectors was first proposed by Shepherd et al. [1] in heterojunction structures. Due to the recent advances in epitaxial growth technology, up to now, several types of internal photoemission infrared (IR) detectors have been proposed and demonstrated [2]. Among them, one important type is metal-semiconductor Schottky barrier IR detectors, such as the most highly developed PtSi/Si detectors [3] operating in the 3–5 μm range. Another important type is semiconductor heterojunction IR detectors, such as GeSi/Si detectors [4,5] developed for the 8–14 μm range. The degenerate Si homojunction detectors [6,7] have a response in the 1–10 μm range. We have employed the concept of internal photoemission in homojunction structures (p^+–p^- or n^+–n^-) under forward bias for FIR [8–13] detection, which is necessary for space astronomy applications of greater than 50 μm.

The detection mechanism of HIWIP detectors involves infrared absorption in the highly-doped emitter layers mainly by free carrier absorption followed by the internal photoemission of photoexcited carriers across the junction barrier and then collection.

* Corresponding author.

[1] Present address: EG&G Judson, 221 Commerce Drive, Montgomeryville, PA 18936, USA.

1350-4495/97/$17.00 © 1997 Elsevier Science B.V. All rights reserved.
PII S1350-4495(97)00006-6

The detector cutoff wavelength λ_c is determined by the interfacial barrier height Δ, as λ_c (μm) = 1.24/Δ (eV), which is a function of device parameters and applied bias. Our modeling studies [11,12,14] have shown that high performance and wavelength tunability in HIWIP FIR detectors could be realized if the emitter layer is doped above the metal-insulator (Mott) transition value but below the critical value at $\Delta = 0$. The recent rapid development of GaAs based long-wavelength quantum well focal plane array cameras make GaAs a promising candidate for developing HIWIP FIR detectors. We have successfully demonstrated the first fabrication of GaAs HIWIP FIR detectors using thin, highly doped p^+ and undoped p^- multilayers [13]. The thin emitter layer yields high internal quantum efficiency due to the low inelastic hole–hole and hole–phonon scattering, and the high doping concentration facilitates strong free carrier absorption, while multilayer structures are used to further increase the quantum efficiency due to the increased photon absorption efficiency and possible photocurrent gain enhancement [9].

However, some optical and electrical properties of the GaAs HIWIP FIR detectors, such as the free carrier absorption, the basic absorption mechanism and photoconductivity behavior under different biases, which are clearly very important for device performance from their detection mechanism, have not yet been studied in detail. An improved understanding of their optoelectronic properties would help in the device development. In this paper, we focus on the spectroscopic study of GaAs HIWIP FIR detectors.

2. Experiment

The GaAs FIR HIWIP detector sample was grown by MBE technique with the substrate temperature of 560°C. The MBE epilayers consist of a 4000 Å bottom contact (p^{++}) layer, a 1500 Å undoped (p^-) layer, 10 periods of thin emitter (p^+) layers (thickness of 150 Å) and undoped p^- layer (thickness of 1000 Å), and finally a 3000 Å top emitter layer and top contact layer as shown in Fig. 1(a), together with its energy band diagram under forward bias (b). The emitter layers were doped with Be to 3×10^{18} cm^{-3} near the Mott transition value [11]. The top and bottom contact layers were doped to $(2–3) \times 10^{19}$ cm^{-3} far above the Mott transition value to ensure an ohmic contact. Good control of MBE growth is indicated by secondary ion mass spectroscopy (SIMS) measurements (see Fig. 2). The contact was formed by deposition of Ti–Pt–Au and the optical window area (A_0) is 260×260 μm^2. The GaAs HIWIP FIR detector was characterized by current–voltage (I–V) measurements and photoresponse. The responsivity was obtained using a Perkin-Elmer, system 2000, Fourier transform infrared spectrometer (FTIR) and a Si composite bolometer as the reference. The absorption of the emitter layer p^+ GaAs thin films was studied by transmission and reflection (near normal

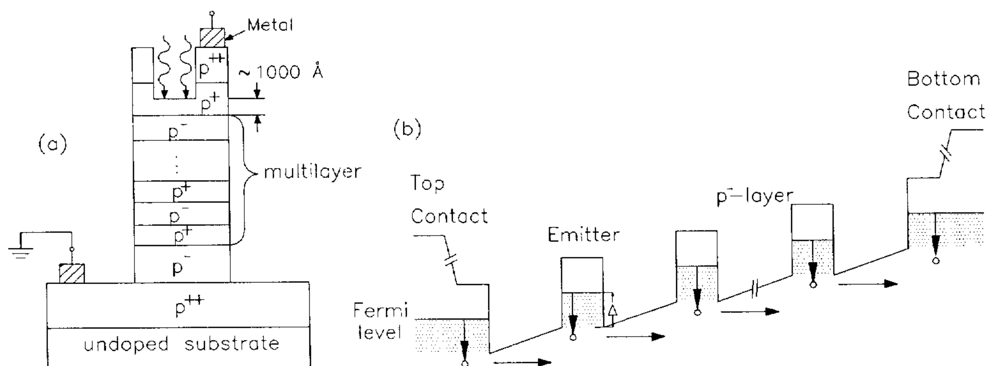

Fig. 1. (a) Schematic of the multilayer HIWIP detector after device processing. p^{++}, p^+ and p^- are the contact layer, emitter layer and undoped layer, respectively. A window is opened on the top side for frontside illumination. (b) Energy-band diagram of the detector under forward bias.

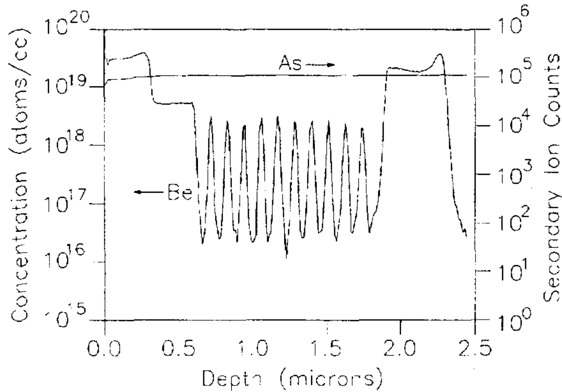

Fig. 2. SIMS profile of the Be doped p-GaAs HIWIP 10-layer detector sample, indicating good control of multilayer interfaces in MBE growth. The background of As is near 10^5 atoms/cm^3.

incidence configuration) of a reference thin film also with the same FTIR system.

3. Results and discussion

From the HIWIP detection mechanism, we can see that the free carrier absorption plays a very important role in the detector performance. Although the free carrier absorption in p-GaAs has been widely studied in the literature, it is limited to the relatively short wavelength range (≤ 20 μm) [15,16]. No previous free carrier absorption measurements have been reported for the wavelength range ≥ 50 μm, where our HIWIP FIR detectors usually work.

In order to understand the FIR free carrier absorption in the p^+-GaAs emitter layers, we have measured the transmission and reflection for a reference thin film. The absorption (A) in thin film is determined from the transmission (T') and reflection (R) in conjunction with the expression

$$A = 1 - T' - R \qquad (1)$$

and further subtraction of the absorption of the substrate. The thin film in our study here was grown by the same MBE conditions as the detector sample. The epilayer thickness of the absorption sample is 1000 Å with a Be concentration of 2×10^{19} cm^{-3}. The absorption results of the thin film over the wavelength range from 50 to 200 μm are shown in Fig. 3. The experimental curve is smoothed to reduce the large modulation and noise which are mainly due to the weak energy in the FIR range and weak response of the TGS detector in that range. The measured values of absorption were found to be almost independent of wavelength, which is similar to the cases of Schottky barrier IR detector samples beyond the lattice bands [17] and GeSi layers above 15 μm [18].

The theoretical absorption curve shown in Fig. 3 was calculated from the complex dielectric constant of the GaAs layer by matching electric and magnetic fields at the interfaces [19]. The dielectric constant of the thin film is derived from the frequency-dependent conductivity for free carriers by

$$\sigma = \frac{\sigma_0}{1 - i\omega\tau} \qquad (2)$$

where σ_0 is the dc conductivity and τ is the relaxation time, which is independent of frequency ω in the semiclassical transport theory. Since our main interest is in the FIR range (≥ 50 μm), the other contributions, e.g., intervalence band transitions and lattice vibrations, are ignored. The carrier concentration is estimated from the doping level, while the relaxation time used is 1.7×10^{-14} s as measured for a sample with similar doping level [16]. The reasonably good agreement between the experimental and theoretical results strongly demonstrates that

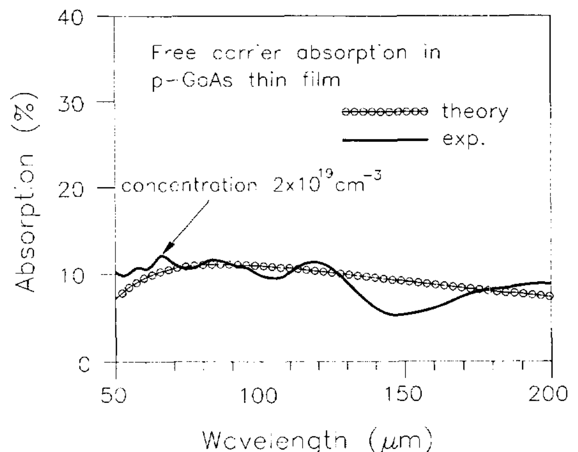

Fig. 3. Experimental FIR free carrier absorption in a p-GaAs thin film with the thickness of 1000 Å and doping concentration of 2×10^{19} cm^{-3} at room temperature (solid curve). The curve has been smoothed with the noise level of 5%. The circles indicate the calculated results.

the absorption is actually due to the contribution of free carriers. The absorption coefficient a can be calculated to be 2.3×10^4 cm^{-1} at 75 μm from

$$\alpha = \frac{1}{d}\ln\left(\frac{1-R}{T'}\right) \tag{3}$$

where d is the layer thickness. The large value of the absorption coefficient in the FIR range is very suitable for our HIWIP detectors, since the absorption coefficient varies very little with temperature due to the almost invariant carrier concentration and mobility with temperature. Furthermore, our experiments also show that the absorption coefficient increases with the doping concentration, which means highly doped emitter layers are more attractive for higher quantum efficiency in HIWIP detectors. This has been demonstrated in our experimental results [13]. However, the dark current can also increase due to higher concentrations. Further work is needed to obtain the relationship between the absorption coefficient and doping concentration.

Next, we study the basic absorption mechanism of free carriers in the detectors. Fig. 4 shows the spectral responses of the GaAs HIWIP FIR detector measured at 4.2 K under low forward biases. A wide

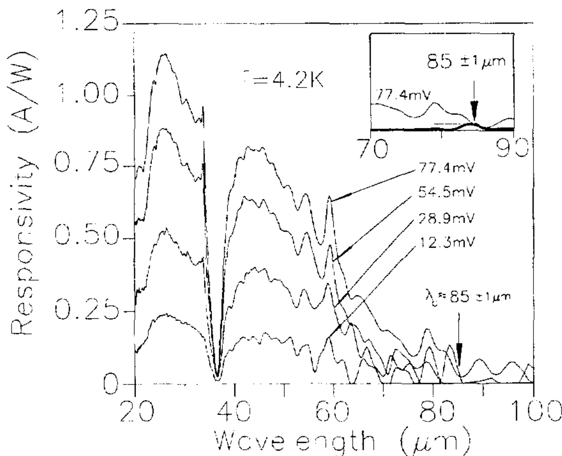

Fig. 4. Spectral response of the GaAs HIWIP FIR detector measured at 4.2 K under different forward bias values ranging from 12.3 mV to 77.4 mV. The deep valley at 36.5 μm is due to the transverse optical (TO) phonons of GaAs. The cutoff wavelength is determined as the level where the signal (thin curve in the inset) reaches the noise level, i.e., standard deviation (thick curve in the inset) of 8 spectra taken under the same conditions.

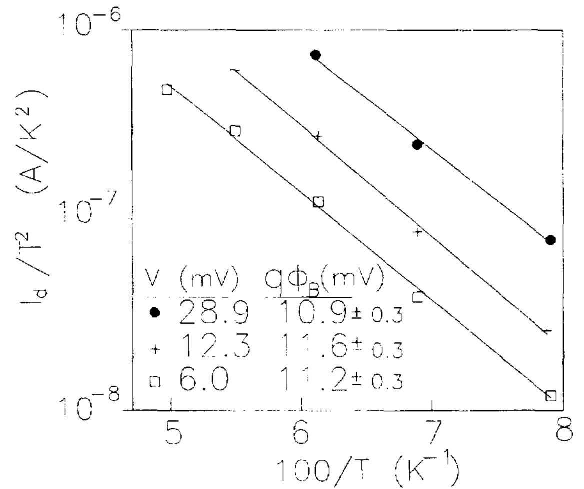

Fig. 5. Plot of I_d/T^2 versus $100/T$ at forward bias of 28.9 mV, 12.3 mV and 6.0 mV, indicating a thermal potential barrier, $q\phi_B$, of 10.9 ± 0.3 mV, 11.6 ± 0.3 mV, and 11.2 ± 0.3 mV, respectively.

spectrum with high responsivity is obtained with the peak quantum efficiency of ~ 5.5% at a bias of 77.4 mV (the peak quantum efficiency of this detector at a bias of 193.2 mV is 9.2%). Increased quantum efficiency can be attributed to the multilayer enhancement effect and possibly due to the phonon gain mechanism [9]. The deep valley at 36.5 μm can be attributed to the transverse optical (TO) phonons, since it corresponds well to the energy of to phonons in GaAs [20]. The long tailing behavior in the long wavelength region reflects the nature of internal photoemission. The cutoff wavelength is determined to be about 85 μm at low biases, corresponding to the interfacial barrier height Δ of 14.6 meV. The cutoff wavelength is determined as the level where the signal reaches the noise level (standard deviation of curve) of the spectrum as seen in the inset of Fig. 4. The bias dependence of the cutoff wavelength has been discussed elsewhere [13]. The effective barrier height of the HIWIP detector can also be determined by using an activation energy analysis of the thermionic current. The thermionic emission (dark) current (I_d) is given by

$$I_d \propto T^2 \exp\left(-\frac{q\phi_B}{k_B T}\right) \tag{4}$$

where T is the absolute temperature, k_B is the Boltzmann constant, and $q\phi_B$ is the thermal potential barrier height above the Fermi level. We have

measured the detector dark I–V characteristics down to 1.6 K and found the dark current has a strong temperature dependence above 12 K. Fig. 5 shows the plot of I_d/T^2 versus $100/T$ for the detector under three small forward bias values of 6.0 mV, 12.3 mV, and 28.9 mV. A good fit is obtained with the value $q\phi_B$ of 10.9 meV, 11.6 meV, and 11.2 meV, respectively.

The optical barrier height Δ determined by spectral response measurements is usually larger than the thermal potential barrier $q\phi_B$ [2]. The discrepancy results mainly from the energy loss of the photoexcited carriers by inelastic scattering prior to the carrier emission. On the other hand, this difference can help us to identify the free carrier absorption mechanism in detectors. The very small energy difference (~ 3 meV) in our detector shows that the photoexcited holes suffer less inelastic scattering in the emitter layers and the free carrier absorption mechanism in our GaAs HIWIP FIR detectors is an acoustic phonon-emission assisted process, rather than the optical phonon-emission assisted process in GeSi/Si structures [21] at 80 K, since our detector is operated at very low temperature. This result also indicates that the GaAs HIWIP FIR detector is an efficient detector, suitable for FIR detection.

Now, we turn the attention to the bias dependence of the responsivity. Our experimental results in Fig. 4 show that the responsivity increases significantly with increasing bias. This dependence is due to the increase of barrier collection efficiency, resulting from the image force effects [11]. However, our experiments also show that the responsivity has a tendency to saturate in the high bias range (near 200 mV in the present detector sample). The above experimental results can be well explained by considering the behavior of photo-excited excess carriers in the emitter layers of the structure.

The physical processes that influence the variation of the excess carrier concentration (also determine the magnitude of photoconductivity signal) are the processes of photoexcitation, capture and thermal radiation. The rate equations for photoionization carriers can be expressed as:

$$\frac{\mathrm{d}p}{\mathrm{d}t} = \sigma_p J p_I - \beta_p p(P_I - p_I), \qquad \frac{\mathrm{d}p_I}{\mathrm{d}t} = -\frac{\mathrm{d}p}{\mathrm{d}t} \tag{5}$$

where σ_p is the photoionization cross section related with the free carrier absorption, J is the light intensity, p_I is the number density of holes in an impurity band with density of P_I, and β_p is the capture cross section for holes related to the internal quantum efficiency of the detector. In the above equations, we have ignored the contribution from thermal radiation, since our detectors are operated at very low temperatures. The rate equation for excess carriers under photoexcitation is then given by:

$$\frac{\mathrm{d}\Delta p}{\mathrm{d}t} = -\frac{\mathrm{d}\Delta p_I}{\mathrm{d}t} = \sigma_p J(p_{I_0} - \Delta p) - \beta_p \Delta p(P_I - p_{I_0} + \Delta p) \tag{6}$$

where p_{I_0} is the number density of holes without photoexcitation. Under steady conditions, the photoexcited excess hole concentration can be approximately written as:

$$\Delta p_{st} = \frac{\sigma_p J p_{I_0}}{\sigma_p J + \beta_p(P_I - p_{I_0})}. \tag{7}$$

As we know, the barrier collection efficiency increases (hence the total internal quantum efficiency increases) with the increasing bias [11], resulting in a decrease in the capture cross section. Therefore, the photoconductivity signal (responsivity) of the detector increases with the bias. However, the term $\sigma_p J$ will dominate the denominator of Eq. (7), i.e. $\sigma_p J \gg \beta_p(P_I - p_{I_0})$, due to the very small capture cross section under high bias conditions, and the photo-excited excess hole concentration Δp_{st} saturates:

$$\Delta p_{st} = \frac{\sigma_p J p_{I_0}}{\sigma_p J} \equiv p_{I_0}. \tag{8}$$

It is obvious that the saturation bias is related with the device parameters, e.g., emitter layer thickness, doping concentration and number of emitter layers etc.

Finally, we estimated the detectivity D_λ^* of our GaAs HIWIP FIR detector from the measured responsivity and dark current. The D_λ^* is estimated by [22]

$$D_\lambda^* = R_\lambda \sqrt{A_0 \Delta f} / i_n, \tag{9}$$

where R_λ is the responsivity, Δf is the bandwidth, and i_n is the dark current noise, which is given by

$$i_n = \sqrt{4qI_d g \Delta f}. \tag{10}$$

Our detector shows a broad spectrum (25–50 μm except for the phonon-induced deep valley region) with $D_\lambda^* \approx 8.4 \times 10^9$ cm $\sqrt{\text{Hz}}$/W at 4.2 K under forward bias of 28.9 mV by assuming a unit photoconductivity gain ($g = 1$). The predicted D_λ^* value for this structure can be $\sim 7 \times 10^{10}$ cm $\sqrt{\text{Hz}}$/W [12]. The relatively low detectivity is due to the existence of large leakage current, which can be observed clearly in the low temperature (below 12 K) I–V measurements. This is not surprising at all, since no guard ring is used in the detector structure, which is widely used in Schottky-barrier and GeSi/Si detectors to suppress the edge leakage [2,4]. We can anticipate a much higher detectivity by using the guard ring. Further attempts to enhance the detectivity can be made by use of an antireflection coating or an optical cavity to increase the internal photoemission efficiency.

4. Conclusion

We have investigated the free carrier absorption and its absorption mechanism in GaAs homojunction interfacial workfunction internal photoemission (HIWIP) far-infrared detectors. Both the strong free carrier absorption and acoustic phonon-emission assisted process indicate that the GaAs HIWIP detector is an efficient detector, suitable for FIR detection. The bias dependence of the responsivity has been explained by rate equations. The detectivity has also been estimated and the relatively low detectivity is attributed to the leakage due to the lack of a guard ring in the detector. Further studies are needed to obtain the relationship between the free carrier absorption coefficient and doping concentration, and to optimize the device performance.

Acknowledgements

This work was supported in part by the NSF under grant #ECS-94-12248. The authors would like to acknowledge P. Chow-Chong, P. Marshall and S.J. Rolfe at NRC for sample fabrication and SIMS measurements, respectively, and S.G. Matsik at GSU for his technical help.

References

[1] F.D. Shepherd, V.E. Vickers and A.C. Yang, U.S. Patent No. 3,603,847 (Sept. 1971).
[2] F.D. Shepherd, Proc. SPIE 1735 (1992) 250.
[3] W.F. Kosonocky, Proc. SPIE 1685 (1992) 2.
[4] T.L. Lin and J. Maserjian, Appl. Phys. Lett. 57 (1990) 1422.
[5] B.Y. Tsaur, C.K. Chen and S.A. Marino, Proc. SPIE 1540 (1991) 580.
[6] S. Tohyama, A. Tanabe and N. Teranishi, IEEE Trans. Electron Dev. 41 (1994) 1535.
[7] T.A. Temofonte, T.T. Braggins, P.R. Emtage, M.J. Bevan, R.N. Thomas, H.C. Nathanson, J. Halvis, R.R. Shiskowski, T.E. Wilson and D.H. McCann, IEEE IEDM Tech. Dig. 121 (1992).
[8] D.D. Coon, R.P. Devaty, A.G.U. Perera and R.E. Sherriff, Appl. Phys. Lett. 55 (1989) 1738.
[9] A.G.U. Perera, J.-W. Choe, M.H. Francombe, R.E. Sherriff and R.P. Devaty, Superlattices Microstruct. 14 (1993) 123.
[10] A.G.U. Perera, R.E. Sherriff, M.H. Francombe and R.P. Devaty, Appl. Phys. Lett. 60 (1992) 3168.
[11] A.G.U. Perera, H.X. Yuan and M.H. Francombe, J. Appl. Phys. 77 (1995) 915.
[12] H.X. Yuan and A.G.U. Perera, Appl. Phys. Lett. 66 (1995) 2262.
[13] A.G.U. Perera, H.X. Yuan, S.K. Gamage, W.Z. Shen, M.H. Francombe, H.C. Liu, M. Buchanan and W.J. Schaff, J. Appl. Phys. 81 (April 1997).
[14] H.X. Yuan and A.G.U. Perera, J. Appl. Phys. 79 (1996) 4418.
[15] R. Braunstein, E.O. Kane, J. Phys. Chem. Solids 23 (1962) 1423.
[16] M.L. Huberman, A. Ksendzov, A. Larsson, R. Terhune and J. Maserjian, Phys. Rev. B. 44 (1991) 1128.
[17] C.K. Chen, B.-Y. Tsaur and M.C. Finn, Appl. Phys. Lett. 54 (1989) 310.
[18] T.L. Lin, J.S. Park, S.D. Gunapala, E.W. Jones and H.M. Del Castillo, Opt. Eng. 33 (1994) 716.
[19] O.S. Heavens, Optical properties of thin solid films (Dover Publications, INC, New York, 1965) ch. 4.
[20] J.S. Blakemore, J. Appl. Phys. 53 (1982) R123.
[21] H.C. Liu, L.J. Li, J.-M. Baribeau, M. Buchanan and J.G. Simmons, J. Appl. Phys. 71 (1992) 2039.
[22] B.F. Levine, A. Zussman, S.D. Gunapala, M.T. Asom, J.M. Kuo and W.S. Hobson, J. Appl. Phys. 72 (1992) 4429.